Insulin Gene Mutations Resulting in Early-Onset Diabetes: Marked Differences in Clinical Presentation, Metabolic Status, and Pathogenic Effect Through Endoplasmic Reticulum Retention

Gargi Meur,[1] Albane Simon,[2] Nasret Harun,[1] Marie Virally,[3] Aurélie Dechaume,[4] Amélie Bonnefond,[4] Sabrina Fetita,[5] Andrei I. Tarasov,[1] Pierre-Jean Guillausseau,[3] Trine Welløv Boesgaard,[6] Oluf Pedersen,[6,7,8] Torben Hansen,[6,9] Michel Polak,[2] Jean-François Gautier,[5] Philippe Froguel,[4,10] Guy A. Rutter,[1] and Martine Vaxillaire[4]

OBJECTIVE—Heterozygous mutations in the human preproinsulin (*INS*) gene are a cause of nonsyndromic neonatal or early-infancy diabetes. Here, we sought to identify *INS* mutations associated with maturity-onset diabetes of the young (MODY) or nonautoimmune diabetes in mid-adult life, and to explore the molecular mechanisms involved.

RESEARCH DESIGN AND METHODS—The *INS* gene was sequenced in 16 French probands with unexplained MODY, 95 patients with nonautoimmune early-onset diabetes (diagnosed at <35 years) and 292 normoglycemic control subjects of French origin. Three identified insulin mutants were generated by site-directed mutagenesis of cDNA encoding a preproinsulin–green fluorescent protein (GFP) (C-peptide) chimera. Intracellular targeting was assessed in clonal β-cells by immunocytochemistry and proinsulin secretion, by radioimmunoassay. Spliced XBP1 and C/EBP homologous protein were quantitated by real-time PCR.

RESULTS—A novel coding mutation, L30M, potentially affecting insulin multimerization, was identified in five diabetic individuals (diabetes onset 17–36 years) in a single family. L30M preproinsulin-GFP fluorescence largely associated with the endoplasmic reticulum (ER) in MIN6 β-cells, and ER exit was inhibited by ~50%. Two additional mutants, R55C (at the B/C junction) and R6H (in the signal peptide), were normally targeted to secretory granules, but nonetheless caused substantial ER stress.

CONCLUSIONS—We describe three *INS* mutations cosegregating with early-onset diabetes whose clinical presentation is compatible with MODY. These led to the production of (pre)proinsulin molecules with markedly different trafficking properties and effects on ER stress, demonstrating a range of molecular defects in the β-cell. ***Diabetes*** **59:653–661, 2010**

Misfolding of insulin, and consequently defective trafficking to secretory granules, has been recognized for a number of years as the likely underlying cause of β-cell dysfunction and death in several rodent models of nonimmune diabetes. These include the *Akita* mouse (1,2), in which a heterozygous mutation in the *Ins2* gene (CA7Y) disrupts interchain disulphide bond formation leading to the engorgement of the endoplasmic reticulum (ER) with misfolded proteins and ER stress. A similar mechanism appears to pertain to the diabetic *munich* mouse, in which intrachain disulphide bond formation is blocked by a C95S mutation (3).

Mutations in the human preproinsulin (*INS*) gene were first identified more than 20 years ago (4–6) and although some of these led to hyperproinsulinemia (7), none was found to be associated with frank diabetes (4–7). More recently, Støy et al. (8) described a group of patients presenting with permanent neonatal diabetes or early infancy–onset diabetes (median age at diagnosis of 13 weeks) who were carriers of a missense *INS* mutation. Most of these mutations were novel, and three were inherited in an autosomal dominant manner. Subsequently, we and three other reports (8–11) described additional *INS* mutations linked to permanent neonatal diabetes or nonautoimmune early infancy–onset diabetes. The majority, although not all, of the mutations led to diabetes onset in the first 6 months of life (8–11). In vitro analyses by Colombo et al. revealed that six of the mutations identified led to ER retention in HEK293T cells and to mild ER stress and at least two led to apoptosis (12).

Some of the *INS* mutations, including R6C (9) and A23S (13) in the signal peptide, R46Q in the B chain, and R55C at the B/C junction (11), were described with later ages at diagnosis (up to 20 years), and these are presumed also to cause insulin misfolding with consequent ER retention, an unfolded protein response (UPR), and ER stress (2). Of note, two individuals with the R55C mutation were diagnosed with diabetes at ages 10 and 13 years, both with

From the [1]Section of Cell Biology, Division of Medicine, Imperial College London, London, U.K.; the [2]Universite Paris Descartes, INSERM U845, Pediatric Endocrinology, Hopital Necker Enfants Malades Paris, Paris, France; the [3]Department of Endocrinology and Diabetes, Lariboisière Hospital, University Paris-Diderot Paris-7, Paris, France; the [4]Centre National de la Recherche Scientifique-UMR8090, Lille Institute of Biology, Lille 2 University, Pasteur Institute, Lille, France; the [5]Department of Endocrinology and Diabetes, Clinical Investigation Center CIC9504, Saint-Louis Hospital, INSERM, U872, University Paris-Diderot Paris-7, Paris, France; the [6]Hagedorn Research Institute and Steno Diabetes Center, Gentofte, Denmark; the [7]Faculty of Health Science, University of Aarhus, Aarhus, Denmark; the [8]Institute of Biomedical Sciences, University of Copenhagen, Copenhagen, Denmark; the [9]Faculty of Health Sciences, University of Southern Denmark, Odense, Denmark; and the [10]Genomic Medicine, Hammersmith Hospital, Imperial College, London, U.K.

Corresponding authors: Guy A. Rutter, g.rutter@imperial.ac.uk, or Philippe Froguel, froguel@mail-good.pasteur-lille.fr.

Received 27 July 2009 and accepted 24 November 2009. Published ahead of print at http://diabetes.diabetesjournals.org on 10 December 2009. DOI: 10.2337/db09-1091.

A.S., N.H., and M.V. contributed equally to this work.

severe clinical symptoms including hyperglycemia and ketoacidosis, but abundant circulating C-peptide levels were detected in each case subject (11). The impact of these mutations on protein folding, ER stress, and β-cell death has, until now, not been examined.

In this study, we aimed to determine the prevalence and phenotype of *INS* mutations that may lead to diabetes at a later age, including in maturity-onset diabetes of the young (MODY), or in patients presenting with nonautoimmune diabetes in mid-adult life (14). We describe here three families with two novel and one previously described *INS* mutations. The L30M mutation is predicted by structural analysis in silico to be better tolerated within the insulin hexamer than a previously described mutation at this residue (L30P), which causes severe diabetes within the first 6 months of life (12). Thus, the L30M mutation was associated with relatively mild diabetes (age at diagnosis in the proband: 17 years). By confocal imaging of chimeric insulin-GFP constructs in which *GFP* is fused in-frame with C-peptide (plasmid hProCpepGFP) (15), we show that this mutation causes clear insulin retention in the ER and concomitant ER stress. By contrast, insulin-GFP bearing the R6H mutation in the signal peptide exited the ER normally and was properly targeted to secretory granules, but induced significant ER stress. The previously reported R55C mutation (11), described here in a MODY family, was also substantially retained in the ER in clonal β-cells. These findings reveal an unexpected divergence in the effects of *INS* mutations at the molecular and cellular level, with the clinical presentation and the severity of the disease.

RESEARCH DESIGN AND METHODS

Subjects and mutation identification. We studied 16 probands of French families with clinically defined MODY based on two criteria: diabetes diagnosed before age 25 years (range of age at diagnosis: 15–23) without requirement of exogenous insulin in the first 2 years, and an autosomal dominant inheritance of type 2 diabetes (16). Of the 16 probands, 15 were negative for a *GCK*/MODY-2 or *HNF1A*/MODY-3 mutation, and 8 were negative for mutations in *HNF4A*/MODY-1, *PDX1*/MODY-4, and *NEUROD1*/MODY-6, which were very rarely found in French MODY patients (16). All patients with unexplained MODY were also negative for serologic markers of type 1 diabetes. Ninety-five patients diagnosed with nonautoimmune diabetes before age 35 years, and presenting with at least one affected first-degree relative (all are Caucasian and of French origin), were included in the study for mutation identification. In addition, we report functional studies on a R6H mutation that was identified among 48 Danish patients with early-onset diabetes and known vertical transmission of the disease (all tested negative for a *HNF4A*/MODY-1, *GCK*/MODY-2, or *HNF1A*/MODY-3 mutation).

The three exons of the *INS* gene were screened for mutations from genomic DNA of the patients by direct sequencing, as previously described (10).

Additional members in three families (two French and one Danish), for which an *INS* mutation was identified in the proband, were also screened for the mutation (see RESULTS). Normoglycemic control subjects of French origin ($n = 292$) were also sequenced and all were found negative for the identified mutations.

Assessment of clinical data. The clinical features of the patients carrying an *INS* mutation, including age at onset and presentation of diabetes, and information on past and current treatments for diabetes, have been reviewed. In the family FR-AM, two subjects (the diabetic proband and his unaffected mother) have undergone a measurement of body composition by dual energy X-ray absorptiometry, and on a separate occasion, a euglycemic hyperinsulinemic clamp for the measurement of glucose uptake and a graded glucose infusion for measurement of insulin secretory response. The proband's mother, who never developed diabetes and was normoglycemic at last examination (after an oral glucose tolerance test [OGTT] at age 68 years), also underwent an intravenous bolus of arginine at the end of the graded glucose infusion to estimate her maximal insulin secretory capacity. Details of metabolic studies are given in supplementary data, available in an online appendix at http://diabetes.diabetesjournals.org/cgi/content/full/db09-1091/DC1.

Proinsulin construct and generation of mutants. Human preproinsulin cDNA cloned in pTARGET vector containing enhanced green fluorescent protein inserted in the C-peptide was kindly provided by Dr. Peter Arvan (University of Michigan) (15). The single mutations (R6H, R6C, L30M, L30P, and R55C) were inserted using a QuikChange II XL site-directed mutagenesis kit (Stratagene, Agilent Technologies, Richardson, TX).

Proinsulin secretion assay. HEK293 cells (5×10^5/well) seeded on six-well plates were transfected in triplicate with wild-type or mutant *INS* constructs (4 μg/well) using Lipofectamine2000 (Invitrogen, Carlsbad, CA). After 48 h, normal growth media were replaced by 1 ml/well of reduced serum media (Dulbecco's modified Eagle's medium, 2% FBS). After 20 h, human proinsulin was measured in the supernatant by radioimmunoassay (Human Proinsulin RIA; Millipore HPI-15K). Experiments were performed independently three times.

Quantification of transient expression of mRNA and protein. HEK293 cells were seeded and transfected as above. Samples for mRNA or protein expression were collected after 48 h. Total RNA was extracted using Trizol reagent (Invitrogen) and treated with DNA-free reagent (ABI Biosystems, Foster City, CA) to remove any DNA contamination. RNA (2 μg) was reverse-transcribed using High-Capacity cDNA Reverse transcription kit (ABI Biosystems). Real-time PCR was carried out with cDNA (equivalent of 20 ng input RNA) using Power SYBR Green master mix (ABI Biosystems) in a 7500 Fast Real-Time PCR system (ABI Biosystems). All real-time primers (human cyclophilin, insulin, and C/EBP homologous protein [CHOP]/GADD153) were generated using ABI Primer Express 3.0. PCR amplification of human XBP1 (X-box binding protein 1) was carried out with the cDNA equivalent of 100 ng input RNA (see supplementary Table 1 for primer sequences).

For protein extraction, cells were washed twice in ice-cold PBS and lysed in 1% Triton X-100 in PBS containing Complete protease inhibitor cocktail (Roche Diagnostics). Total protein (30 μg/well) was analyzed on 12% SDS–polyacrylamide gels and transferred to polyvinylidene fluoride membranes. Blots were blocked with 5% nonfat milk in Tris-buffered saline for 1 h and, subsequently, incubated 1 h for each, first with primary antibody (monoclonal anti-GFP, 1:1,000 [Sigma clone GSN24], monoclonal anti-α-tubulin, 1:10,000 [Sigma clone B-5–1–2]) followed by horseradish peroxidase–linked secondary antibody (1:10,000; GE Healthcare), with 3× 10-min washes with Tris-buffered saline–0.1% Tween 20 between incubations. Blots were developed using ECL Western blot detection reagent (GE Healthcare Life Sciences) and exposing to Hyperfilm ECL (GE Healthcare Life Sciences).

Immunocytochemistry. MIN6 mouse pancreatic β-cells (17) seeded on poly-L-lysine–coated coverslips were transfected with wild-type or mutant insulin constructs (4 μg/well) with/without plasmid encoding DsRED-ER (2 μg/well; Clontech) using Lipofectamine2000 and were allowed to overexpress for 48 h. Cells coexpressing insulin granule marker were infected with neuropeptide Y (NPY)-Venus virus (100 multiplicity of infection) (18) 24 h after transfection with plasmids. Coverslips were washed twice with PBS, fixed in 4% paraformaldehyde (5 min), washed again, and mounted on slides with Prolong gold (Invitrogen). Apoptosis was measured by staining transfected cells for 5 min with annexin V–phycoerythrin before fixation (Calbiochem, Merck Chemicals, Nottingham, U.K.). Cells were imaged using a Zeiss Axiovert 200M microscope (Carl Zeiss, Jena, Germany) fitted with a PlanApo ×63 oil-immersion objective and a ×1.5 Optivar attached to a Nokigawa spinning disc confocal head. Samples were illuminated using steady-state 488-and 560-nm laser lines and emission was collected through ET535/30 and ET620/60 emission filters (Chroma). Images were captured using a Hamamatsu EM CCD digital camera, model C9100–13, controlled by an Improvision/Nokigawa spinning disc system running Volocity software.

Data analysis and statistics. Statistical significance was estimated using ANOVA with Bonferroni multiple comparison test or paired t tests. Differences with at least $P < 0.05$ were considered statistically significant.

RESULTS

Identification of *INS* mutations and clinical presentation of diabetes. Three heterozygous missense *INS* mutations were identified in two French and one Danish patients diagnosed with nonautoimmune diabetes before age 25 years. No further mutations were found by screening additional French probands with later onset familial diabetes.

One novel mutation, a c.88C>G-p.L30M change, was found in a patient with diabetes diagnosed at 17 years of age of normal body weight. This mutation was not present in 292 nondiabetic control subjects of French origin. Molecular modeling (Fig. 1*A*) revealed that this replace-

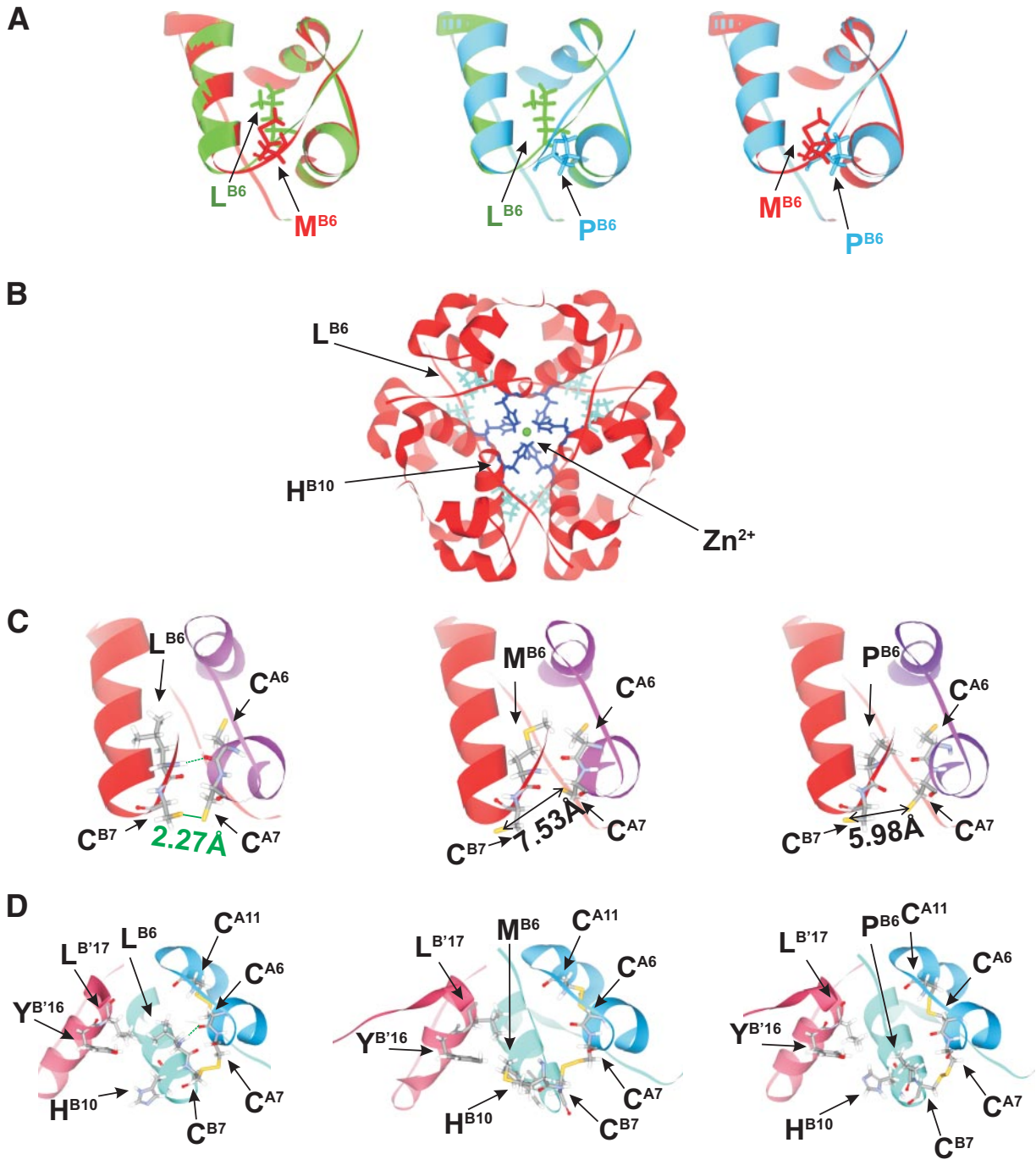

FIG. 1. Modeling of mutant insulin. Impact of L30M and L30P mutations on insulin folding (*A*) and hexamerization (*B* and *C*). *A*: Energy-minimized models of insulin A and B chains, superimposed. (*Left*) wild type, green; L30M, red; (*center*) wild type, green, L30P, blue; (*right*) L30M, red, L30P, blue. Homology models were built using Modeler9v4 software (http://www.salilab.org) using *1mso* human insulin structure as a template (30). *B*: Insulin hexamer showing L30 (L^{B6}) and H34 (H^{B10}) residues and Zn^{2+} (30). *C* and *D*: Close-up showing the impact of L30M ($L^{B6}M$, *center*) and L30P ($L^{B6}P$, *right*) mutations in insulin B-chain versus wild type (*left*) showing the increased Cys-Cys distance, disfavoring disulphide bond formation (*C*), and changes to the structure after disulphide bond formation (*D*). Leucine at position 6 of the B-chain (L30) interacts with cysteine at position 6 of the A chain and leucine 17 and tryptophan 16 of the neighboring B-chain (B′). L30M and L30P mutations would therefore weaken or eliminate the interactions within the monomer and may also affect hexamer formation.

ment in the hydrophobic core of the insulin B chain is more conservative than a previously described mutation at the same site (L30P) (12) but, being located at the dimer interface, may affect insulin multimerization (Fig. 1*B* and *C*, see legend).

At diagnosis, the revealing symptom in the patient was weight loss and the fasting glycemia was 16.5 mmol/l. No autoimmunity against pancreas was detected, and the pancreatic morphology (assessed by abdominal tomodensitometry) was normal. Initially, glycemic control was satisfactory with oral hypoglycemic agents (OHAs; glibenclamide associated to metformin). Subsequently, the association of various oral drugs proved insufficient, and insulin requirement occurred 9 years after diagnosis. A progressive increase in insulin needs was observed during the past 14 years (from 0.45 to 0.83 UI $\cdot$ kg^{-1} $\cdot$ day^{-1}), and A1C

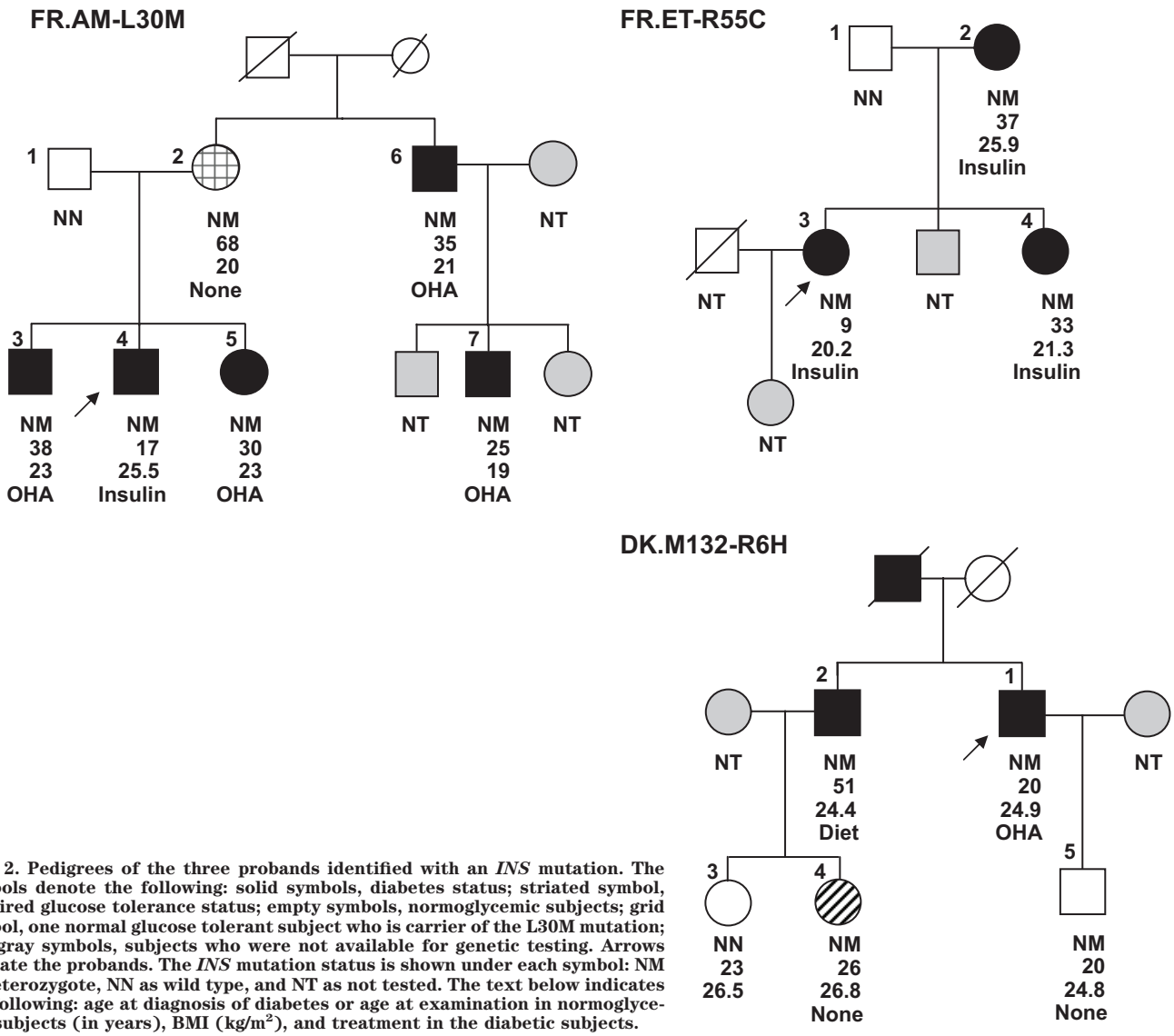

FIG. 2. Pedigrees of the three probands identified with an *INS* mutation. The symbols denote the following: solid symbols, diabetes status; striated symbol, impaired glucose tolerance status; empty symbols, normoglycemic subjects; grid symbol, one normal glucose tolerant subject who is carrier of the L30M mutation; and gray symbols, subjects who were not available for genetic testing. Arrows indicate the probands. The *INS* mutation status is shown under each symbol: NM as heterozygote, NN as wild type, and NT as not tested. The text below indicates the following: age at diagnosis of diabetes or age at examination in normoglycemic subjects (in years), BMI (kg/m^2), and treatment in the diabetic subjects.

ranged from 5.0 to 9.9%. No microangiopathy or macroangiopathy was detected in this patient after 24 years of diabetes evolution.

The L30M mutation cosegregated in five individuals from the proband's family with early-onset diabetes (range of age at diagnosis: 17–38 years; range of BMI at last examination: 19–25.5 kg/m^2; Fig. 2). However, the proband's mother was found to carry the mutation but was not known to be diabetic, and had a normal OGTT at her last examination at age 68 years (fasting and 2-h post–glucose load glycemia of 5.1 and 7.6 mmol/l, respectively). The other diabetic relatives were treated with OHA.

We also identified another MODY proband bearing a c.163C>T-p.R55C mutation at the B/C junction (previously reported in a Norwegian case subject with apparent type 1 diabetes, but negative for autoantibodies [11]). The patient was diagnosed with diabetes at age 9 years by signs of polyuria and polydipsia, which required exogenous insulin therapy at the time of diagnosis. After a follow-up of >50 years, clinical records indicated no signs of late-diabetic complications (absence of retinopathy, nephropathy, or cardiovascular disease) and a stable, well controlled glycemic profile (A1C ranges <6%). The mutation was found to cosegregate with diabetes in two other diabetic relatives, who were diagnosed at ages 37 (the mother) and 33 (the sister) years (Fig. 2). They were initially treated with OHA, then with insulin therapy (12 and 5 years, respectively, after their initial treatment). No complications of diabetes were recorded from clinical evaluations of the sister. The mother of the proband died at age 87 years (the cause of death was not directly related to diabetes).

A c.17G>A substitution, leading to a R6H change in the signal peptide, was identified in a Danish proband (Fig. 2). This patient was diagnosed with mild diabetes at age 20 years. He was treated with diet and OHA since diagnosis. At age 50 years, he was treated with metformin (1 g × 2), A1C was 6.4%, fasting serum C-peptide was 419 pmol/l, and fasting plasma glucose was 6.4 mmol/l. He had developed retinopathy, neuropathy, and microalbuminuria. A brother to the proband (M132–2 on Fig. 2), who also carries the mutation, was diagnosed with diabetes at age 51 years. At age 53 years, he was treated with diet alone and had no signs of late-diabetic complications. A daughter of the brother (M132–4 on Fig. 2), carrying the mutation, was diagnosed with impaired glucose tolerance at age 26 years and with gestational diabetes at age 27. After pregnancy, she was treated with diet alone. She had no signs of diabetes complications.

TABLE 1
Anthropometric and metabolic characteristics of two subjects (diabetic proband and nondiabetic mother from family FR-AM) carrying the L30M-*INS* mutation, compared with a group of control subjects

	Control group	Diabetic proband	Nondiabetic mother
n	18		
Sex ratio (female/male)	10/8	Male	Female
Age at examination (years)	26.8 ± 6.6	40	68
BMI (kg/m^2)	22.9 ± 3.3	25.9	21.7
OGTT			
Fasting blood glucose (mmol/l)	4.6 ± 0.3	7.2	5.1
Blood glucose at 120 min (mmol/l)	5.8 ± 1.3		7.6
Fasting insulin (mUI/l)	5.5 ± 3.8		2.4
Early insulin secretion (mUI/mmol)	16.9 ± 10.7		2.3
Euglycemic hyperinsulinemic clamp			
Body mass (%)	23.8 ± 7.4	18.4	17.1
M value (mg · kg fat free mass^{-1} · min^{-1})	10.9 ± 2.4	9.1	9.4
Graded glucose infusion			
Mean insulin secretion rate (pmol · kg^{-1} · min^{-1})	8.80 ± 3.70	0.66	1.19
Arginine test			
Blood glucose at arginine injection (mmol/l)	20 ± 2.9		25.6
Insulin AUC (mUI × 5 min/l)	1,798.6 ± 1,426.4		43.7
Incremental insulin (AUC insulin in mUI × 5 min/l)	1,122.8 ± 850.5		45.3

Data are means ± SD. The *M* value is an estimate of insulin sensibility during the euglycemic hyperinsulinemic clamp. The control group represents young adult subjects of French origin. AUC, area under the curve.

In vivo metabolic studies in two carriers of the L30M mutation. As shown in Table 1, the diabetic proband (family FR-AM) displayed a dramatic decrease in insulin secretion during graded glucose infusion, whereas insulin sensitivity measured during the euglycemic hyperinsulinemic clamp was normal; this is consistent with β-cell failure as the cause of diabetes. His nondiabetic mother was also found to have a clear defect in insulin secretion, which was apparent in response to both oral and intravenous glucose load and also to the intravenous arginine test during hyperglycemia, raising the question as to why she did not develop diabetes. Blood glucose level at 120 min during OGTT (7.6 mmol/l) was close to the glucose intolerance threshold (7.8 mmol/l). However, insulin sensitivity in this person must be considered high, taking into account her age and her reported high level of physical activity.

Impact of insulin mutations on intracellular trafficking ex vivo. We next examined the ability of the identified mutations to affect insulin exit from the ER, initially using HEK293 cells (12,15). These cells lack a well-defined regulated secretory pathway such that normal ER exit of a proinsulin-GFP chimera (15) leads to the constitutive release into the medium. Along with the three identified mutations (R6H, L30M, R55C), two other previously reported mutations, R6C (9) and L30P (12), were introduced in the preproinsulin-GFP chimera (denoted henceforth as PPI) for comparative molecular studies. Although all the mutants expressed at similar levels to the wild-type at the mRNA level (Fig. 3*A*), expressed protein levels in total cell extract were lower in wild-type and R6H cells, most likely reflecting the more efficient constitutive secretion of these molecules than the other mutant proteins (Fig. 3*B*). All mutant proinsulin proteins migrated to same extent as wild-type proinsulin on reducing SDS-PAGE, indicating efficient cleavage of preproinsulin signal peptide. When secreted proinsulin was measured in the culture media, the L30M mutant displayed a decrease in proinsulin release rate, albeit less marked than that for the L30P mutant (Fig. 3*C*). In contrast, secretion of R6H was not significantly different from wild type, although mutation to cysteine at the same location (R6C) in the signal peptide led to substantially compromised proinsulin release (Fig. 3*C*). The release of the B/C junction mutant proinsulin, R55C, was also considerably reduced (Fig. 3*C*), indicative of ER retention.

A large percentage of L30M (69 ± 8%) and R55C (42 ± 3%) mutant chimera-expressing HEK293 cells displayed a marked difference in the distribution of fluorescence compared with wild-type insulin GFP-expressing cells: whereas fine tubular/reticular fluorescence, reminiscent of a healthy ER (19), was evident in wild-type chimera-expressing cells, a globular, perinuclear staining was usually apparent in cells expressing the L30M or R55C mutant constructs (supplementary Figure 1). This observation is consistent with retention of the mutant chimera in an inflated and engorged ER.

To extend these findings to insulin-secreting cells, we next expressed wild-type or mutant chimeras in clonal MIN6 β-cells (17). The fluorescence of wild-type hProCpepGFP was closely colocalized with the co-overexpressed secretory granule marker, neuropeptide Y-Venus (Fig. 4) (18), with little or no colocalization with the overexpressed ER marker, DsRed-ER (Fig. 5*A*). The insulin-GFP fluorescence distribution profile along a straight line drawn across one of the middle sections of individual cells in Fig. 5*A* generates large peaks with intervals of low fluorescence zones (Fig. 5*B*), implying compacted storage of protein in dense core vesicles and a lack of significant retention in the ER. By contrast, L30M chimera fluorescence was barely detected in the NPY-Venus–positive compartment (Fig. 4) but was strongly colocalized with DsRed-ER, confirming large-scale retention in the latter organelle (Fig. 5*A*). The distribution of L30M was very close to the structurally most perturbing mutation, L30P (Fig. 1). On the other hand, R6H or R6C mutations in the preproinsulin signal peptide appeared to exert no untoward effects on proper folding within the ER (Fig. 5*A*), as implied by appropriate vesicular targeting (Fig. 4) and as confirmed by a fluorescence profile similar to the wild-type

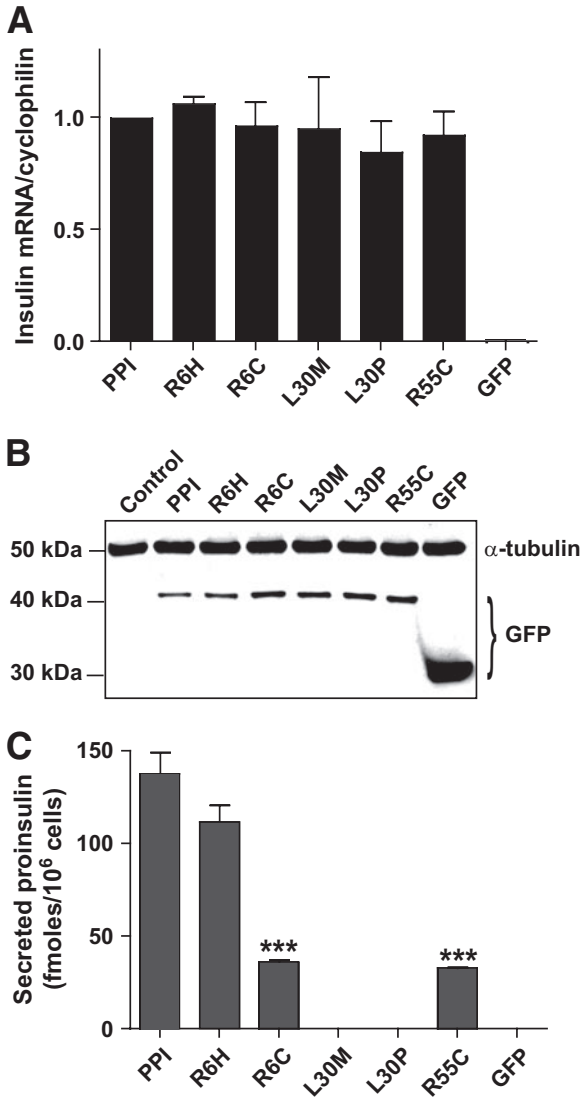

FIG. 3. Impact of insulin mutations on ER release and secretion in HEK293 cells. *A*: Real-time PCR measurements of recombinant human *INS* mRNA expression in transfected HEK293 cells normalized to endogenous cyclophilin (means ± SEM; $n \geq 5$). *B*: Typical Western blot ($n \geq 5$) of total protein (30 μg/lane) from HEK293 cells transfected or not with *INS* constructs separated on 12% reducing SDS-PAGE and probed first with anti-GFP antibody, followed by α-tubulin as loading control. *C*: Secreted proinsulin content in 1 ml media of transfected HEK293 cells collected for a period of 20 h (means ± SEM; $n \geq 5$). No secretion recorded for empty spaces. Data were analyzed by ANOVA with Bonferroni multiple comparison test. ***$P < 0.001$.

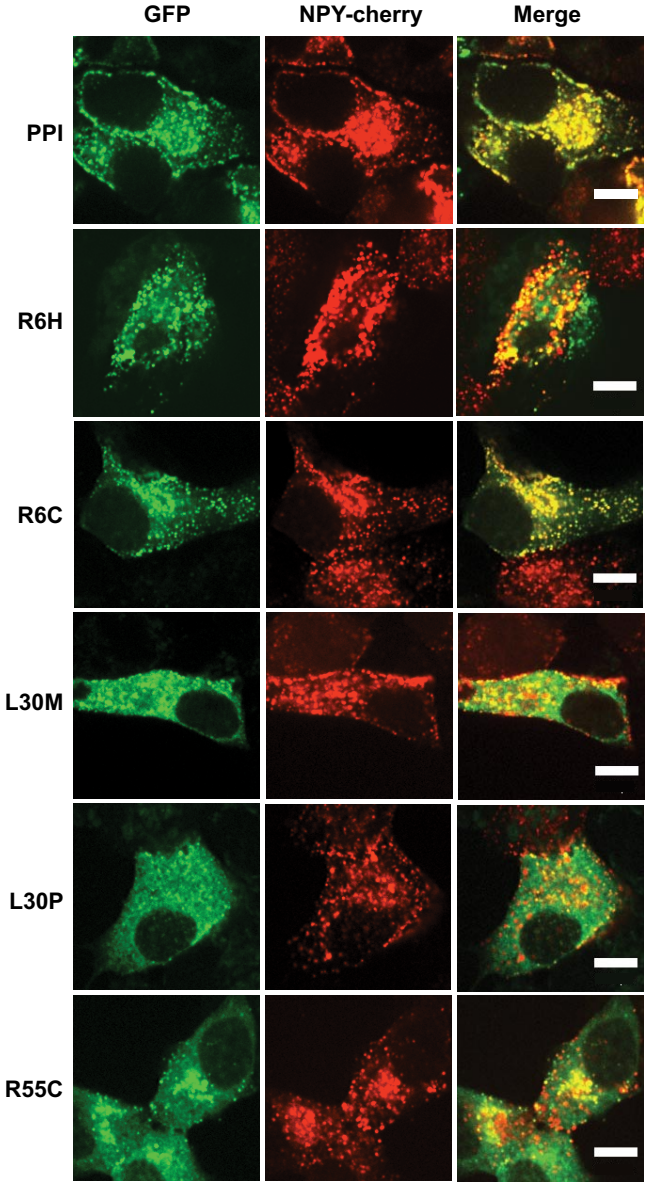

FIG. 4. Subcellular targeting of *INS* mutants to the dense core secretory vesicles. MIN6 β-cells transfected with mutant *INS*-GFP constructs were subsequently (typically after 24 h) infected with adenoviral vector expressing NPY-cherry, a dense core vesicle marker. Protein expression after 48 h was studied under ×63 oil-immersion lens of confocal microscope using 488-and 568-nm laser lines. Images shown are of single cells ($n \geq 25$) with typical distribution of *INS* mutant proteins. Note that the R6H panel captured two overlapping cells expressing the R6H mutant in same focal plane, but only the top one expressed NPY-cherry. Scale bar, 7 μm. (A high-quality digital representation of this figure is available in the online issue.)

chimera (Fig. 5*B*). However, the R55C mutation displayed an altered distribution pattern of insulin chimera with both dense core vesicular targeting (Fig. 4*A*) as well as considerable evidence of ER retention (Fig. 5*A*). The fluorescence distribution profile of L30M and R55C indicated absence of peaks above the cutoff and a diffuse presence throughout the ER (Fig. 5*C*). Furthermore, the total number of cells in a population of MIN6 β-cells that produced mutant insulin-containing granules significantly decreased in the presence of L30M and R55C mutants (Fig. 6), consistent with either complete deficiency in the former or attenuated insulin secretion in the latter (Fig. 3*C*).

Impact of insulin mutations on ER stress. Misfolded client proteins accumulate in the ER to trigger an UPR that initially upregulates ER chaperones but, in the longer term, evokes cell death (20,21). The ER retention of L30P and R55C mutants, a possible result of protein misfolding, prompted us to examine whether they triggered UPR in HEK293 cells by measuring the ER stress markers, XBP1 (12,22) and CHOP/GADD153 (23). Although the ER localized sarco(endo)plasmic reticulum pump blocker, thapsigargin, provoked enormous ER stress (24), indicated by substantial accumulation of spliced XBP1 (Fig. 7*A* and *B*) and CHOP/GADD153 mRNA (Fig. 7*C*), transfection with the L30M, L30P, and R55C mutants also caused a moderate, yet significant increase of ER stress compared with wild-type insulin. Interestingly, ER stress was also observed in cells expressing the R6H mutant, as revealed by enhanced expression of CHOP/GADD153, if not of spliced

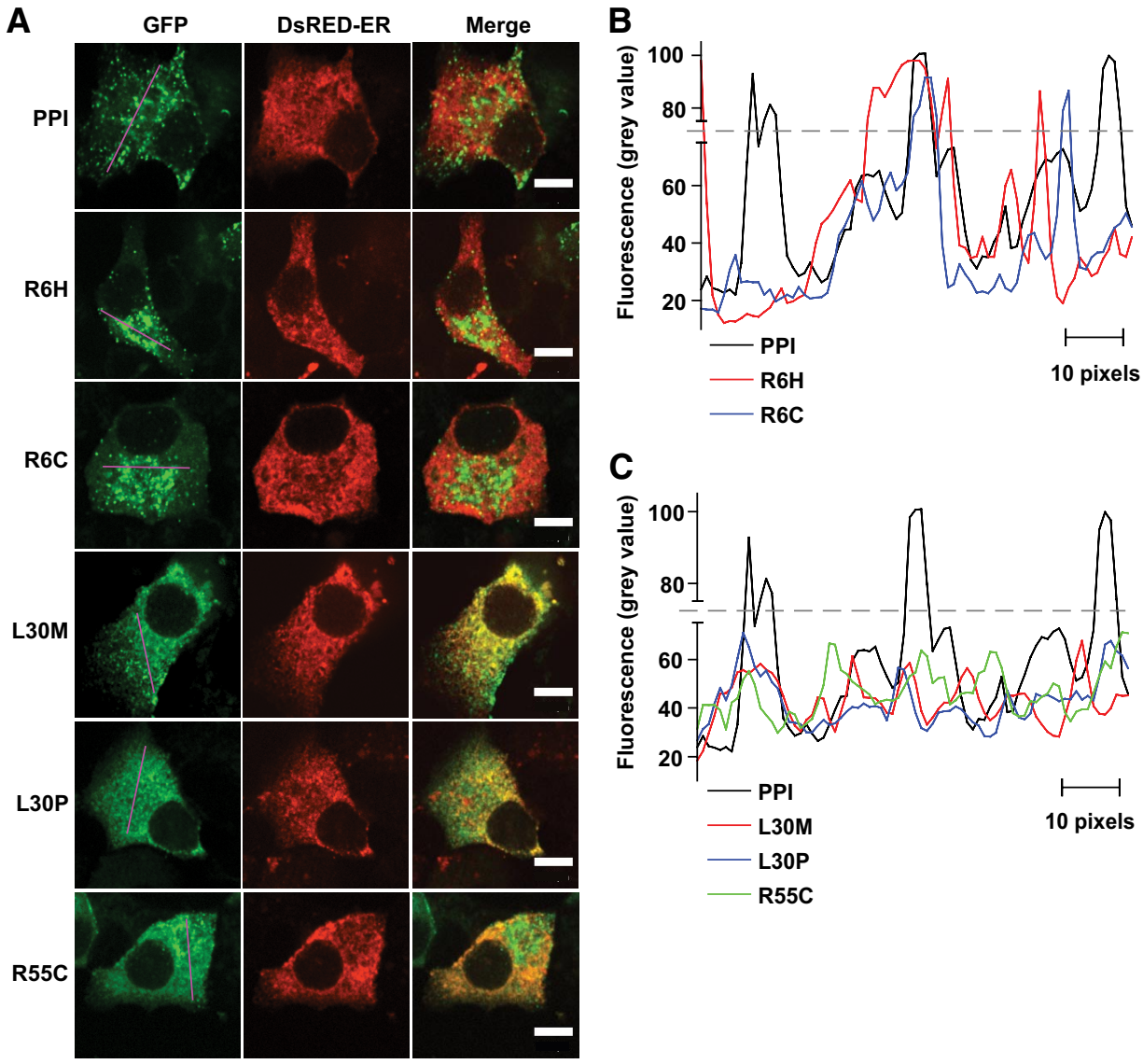

FIG. 5. ER retention caused by *INS* mutations and distribution of *INS*-GFP mutant proteins within single clonal β-cells. *A*: MIN6 β-cells cotransfected with DsRED-ER, an ER marker along with *INS*-GFP constructs and protein expression was studied after 48 h, as in Fig. 4. Scale bar, 7 μm. *B* and *C*: Green fluorescence was measured (in absolute gray values) across a line drawn through middle section of typical transfected MIN6 cells and the profile plotted against distance in pixels. The gray broken line limits a cutoff fluorescence intensity to differentiate local accumulation of high concentrations of insulin in vesicles compared with diffused appearance across ER. (A high-quality digital representation of this figure is available in the online issue.)

XBP1 (Fig. 7*B* and *C*), and despite the fact that only R6H mutant preproinsulin, but not proinsulin or mature insulin, differed from the corresponding wild-type proteins. Despite elevated ER stress marker levels, under these experimental conditions none of the three new mutants evoked any significant apoptotic cell death that could be detected with annexin V staining of HEK293 cells (data not shown).

DISCUSSION

More than 25 separate mutations in the human *INS* gene have been described, leading to very early-onset diabetes diagnosed in the neonatal period or early infancy in most case subjects, but also later in childhood or in young adulthood (25). Our study from two European cohorts of diabetic patients diagnosed with MODY confirms that coding *INS* mutations are also associated with the MODY form of diabetes, albeit with a much lower prevalence compared with the MODY-2/*GCK* and MODY-3/*HNF1A* subtypes. Moreover, our description of three families with three separate mutations highlights a great variability in clinical presentation, as well as in the severity and evolution of diabetes, even between carriers of the same mutation within a family.

Several of the *INS* mutations leading to the most profound pathologies (i.e., neonatal diabetes) involve the appearance of an insulin molecule with an unpaired cysteine residue, as observed in *Akita* (1) and *munich* (3) mice, and cause a severe folding defect, UPR, and β-cell apoptosis. Human *INS* mutations at position 6 of the B-chain, L30P or L30V, have previously been found to cause early-infancy diabetes (12). These mutants were shown to be substantially retained in the ER and lead to abnormal splicing of XBP1, implying a folding defect and an increased ER stress response. However, the behavior and trafficking of these mutants in insulin-secreting cells has not previously been described.

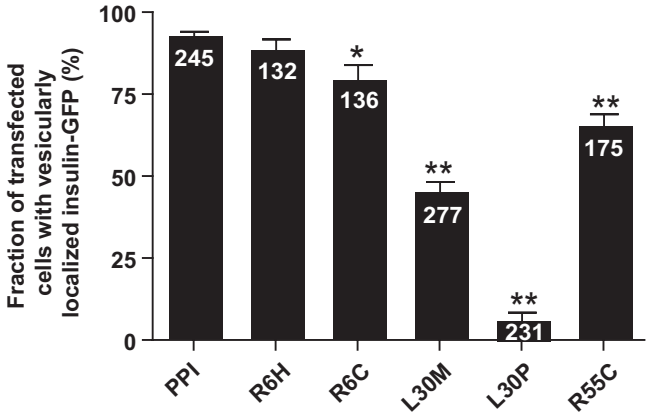

FIG. 6. Quantitation of vesicular targeting of mutant insulin. A representative sample from the population transfected MIN6 β-cells was chosen to count the fraction of cells showing vesicular localization of *INS*-GFP (as determined by GFP colocalization with red NPY-cherry). Bars represent means ± SEM; *n* = numbers on bars of total number of cells counted from three separate experiments. Data were analyzed by ANOVA with Bonferroni multiple comparison test. **P* < 0.05, ***P* < 0.001.

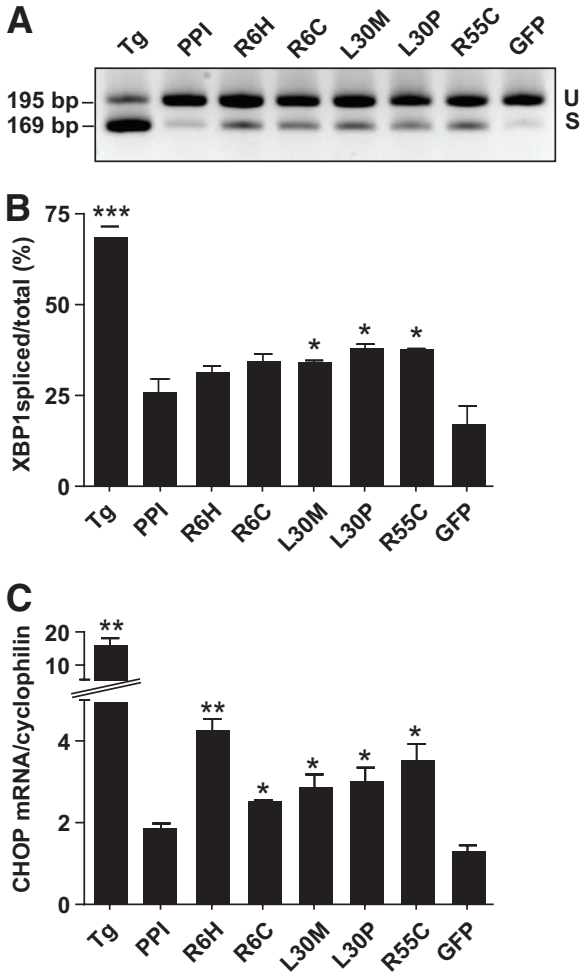

FIG. 7. ER stress markers induced by *INS* mutants. HEK293 cells were either transfected with *INS* mutants allowing 48 h for protein expression or treated with 100 nmol/l thapsigargin (Tg) for 4 h, and total RNA was extracted. After reverse transcription, 2 μg RNA was amplified either by conventional PCR (100 ng cDNA) or by real-time PCR (20 ng cDNA). *A*: Typical agarose gel (2%) separated with Tris-borate-EDTA (TBE) buffer showing spliced (S) and unspliced (U) forms of PCR-amplified XBP1 cDNA. *B*: Quantification of spliced form of XBP1. The gray values of the bands (as in *A*) of spliced and unspliced XBP1 quantified (means ± SEM; *n* = 3). *C*: Real-time quantification of CHOP/GADD153 mRNA normalized to endogenous cyclophilin (means ± SEM; *n* = 3). All data were analyzed by paired *t* tests comparing with wild-type *INS* PPI. **P* < 0.05, ***P* < 0.001.

Interestingly, the L30M replacement, described here as a novel mutation, led to a milder clinical presentation (diabetes onset at 17–38 years) despite clear ER retention and evidence of UPR (Figs. 3–5). Although the presence of a methionine at this site is likely to lead to a smaller change in the structure around the hydrophobic core than proline (Fig. 1*A*), the location of L30 at the dimer-dimer interface (Fig. 1*B* and *C*) might affect the formation of insulin multimers. Although insulin hexamerization and condensation are generally thought to occur in the trans-Golgi and in immature granules, it seems conceivable that defective dimer association may occur earlier in the secretory pathway and hence influence exit from the ER of the mutant. Such a model would be consistent with the L30M mutant prompting a UPR. Importantly, the more substantial vesicular targeting of the L30M than the L30P mutant in MIN6 cells (Fig. 6) suggests that ER exit is more efficient for the former, even though secretion of proinsulin from HEK293 cells was below the level of detection with either mutant (Fig. 3*C*). Nonetheless, this difference presumably permits more sustained insulin secretion in early life for L30M mutant carriers, with less marked β-cell loss and hence a later onset of diabetes than those carrying L30P, and leads to marked phenotypic differences within one family.

Interestingly, the novel mutation R6H barely affected proinsulin release or ER stress, as assessed by XBP1 splicing, and yet prompted the largest induction of CHOP mRNA of all the mutants examined. Because human preproinsulin contains a signal peptide with a classical tripartite domain structure, that is, a positively charged NH_2-terminal (n-), a hydrophobic core (h-), and a COOH-terminal polar domain (c-region), and because the h-and c-regions determine processing of signal peptide (26), the R6H mutation in the n-region should not affect signal peptide cleavage. However, a shift in net positive charge at cellular pH in the n-region due to replacement of arginine (acid dissociation constant, 12.5) by histidine (acid dissociation constant, 6–6.5) may influence both the level of protein translation and efficiency of export (27). This in turn may cause mild ER stress sufficient to prompt CHOP activation (28), perhaps by activating PERK, although IRE1 activity and thus XBP1 splicing are unaffected. Whatever the underlying mechanisms are, these data indicate that this mutation in the preproinsulin signal peptide leads to a distinct form of UPR/ER stress response compared with mutants in the mature insulin molecule, which seems likely to impact on β-cell survival in vivo, as suggested by the clinical presentation of diabetes in the Danish family. The R6H mutant thus acts somewhat differently to the previously described R6C mutation (9) (Fig. 7*C*), causing more limited β-cell loss or dysfunction (29).

Although we cannot exclude the possibility that the behavior of the proinsulin mutants in the cell culture systems used here may differ from that of the mutants in human β-cells in vivo, earlier observations also support the above view that the molecular mechanisms underlying diabetes in carriers of different *INS* mutations may differ. Thus, Molven et al. (11) reported abundant C-peptide in two carriers of the R55C mutation, implying a substantially retained β-cell mass and normal insulin release, despite hyperglycemia and ketoacidosis at presentation. However, split proinsulin may also have contributed to the apparent

C-peptide signal in this earlier study. Because the proinsulin mutant is unlikely to be fully processed by carboxypeptidase E, the presence of an unpaired cysteine may prompt a UPR. Of note, the previously identified R89C mutation at the C-A junction led to a dramatic decrease in C-peptide levels in two patients with neonatal diabetes, suggesting massive β-cell loss (12).

In summary, we show that mutations in the human preproinsulin gene are a cause of nonautoimmune diabetes with variable clinical features at presentation in early life or in young adulthood, and also in the long-term evolution. Our findings suggest that the degree of ER retention, and the nature of the UPR, can differ widely between mutants, generating a range of underlying β-cell defects.

ACKNOWLEDGMENTS

G.A.R. has received grant support from the Wellcome Trust (Programme Grant 081958/2/07/Z), The European Union (FP6 "Save Beta"), the Medical Research Council (G0401641), and the National Institutes of Health (RO1 DK-071962–01). M.P. and M.Va. have received grant support from the French ANR-07-MRAR-018. P.F. has received grant support from the European Union (Integrated Project EuroDia LSHM-CT-2006–518153 in the Framework Programme 6 [FP6] of the European Community). J.-F.G. has received an institutional grant (Programme Hospitalier de Recherche Clinique) from Assistance Publique–Hôpitaux de Paris (in vivo metabolic studies). A.I.T. received a post-doctoral fellowship from the Juvenile Diabetes Research Foundation.

No potential conflicts of interest relevant to this article were reported.

We thank the patients and their families for their participation in this study. We thank Dr. Trevor Biden (Garvan Institute, Sydney, Australia) for advice on ER stress markers and Dr. Peter Arvan (University of Michigan) for the generous gift of hProCpepGFP plasmid.

REFERENCES

1. Wang J, Takeuchi T, Tanaka S, Kubo SK, Kayo T, Lu D, Takata K, Koizumi A, Izumi T. A mutation in the insulin 2 gene induces diabetes with severe pancreatic beta-cell dysfunction in the Mody mouse. J Clin Invest 1999;103:27–37
2. Ron D. Translational control in the endoplasmic reticulum stress response. J Clin Invest 2002;110:1383–1388
3. Herbach N, Rathkolb B, Kemter E, Pichl L, Klaften M, de Angelis MH, Halban PA, Wolf E, Aigner B, Wanke R. Dominant-negative effects of a novel mutated Ins2 allele causes early-onset diabetes and severe beta-cell loss in Munich Ins2C95S mutant mice. Diabetes 2007;56:1268–1276
4. Shoelson S, Fickova M, Haneda M, Nahum A, Musso G, Kaiser ET, Rubenstein AH, Tager H. Identification of a mutant human insulin predicted to contain a serine-for-phenylalanine substitution. Proc Natl Acad Sci U S A 1983;80:7390–7394
5. Shoelson S, Haneda M, Blix P, Nanjo A, Sanke T, Inouye K, Steiner D, Rubenstein A, Tager H. Three mutant insulins in man. Nature 1983;302:540–543
6. Shibasaki Y, Kawakami T, Kanazawa Y, Akanuma Y, Takaku F. Posttranslational cleavage of proinsulin is blocked by a point mutation in familial hyperproinsulinemia. J Clin Invest 1985;76:378–380
7. Yano H, Kitano N, Morimoto M, Polonsky KS, Imura H, Seino Y. A novel point mutation in the human insulin gene giving rise to hyperproinsulinemia (proinsulin Kyoto). J Clin Invest 1992;89:1902–1907
8. Støy J, Edghill EL, Flanagan SE, Ye H, Paz VP, Pluzhnikov A, Below JE, Hayes MG, Cox NJ, Lipkind GM, Lipton RB, Greeley SA, Patch AM, Ellard S, Steiner DF, Hattersley AT, Philipson LH, Bell GI, Neonatal Diabetes International Collaborative Group. Insulin gene mutations as a cause of permanent neonatal diabetes. Proc Natl Acad Sci U S A 2007;104:15040–15044
9. Edghill EL, Flanagan SE, Patch AM, Boustred C, Parrish A, Shields B, Shepherd MH, Hussain K, Kapoor RR, Malecki M, MacDonald MJ, Støy J, Steiner DF, Philipson LH, Bell GI, Neonatal Diabetes International Collaborative Group, Hattersley AT, Ellard S. Insulin mutation screening in 1,044 patients with diabetes: mutations in the INS gene are a common cause of neonatal diabetes but a rare cause of diabetes diagnosed in childhood or adulthood. Diabetes 2008;57:1034–1042
10. Polak M, Dechaume A, Cavé H, Nimri R, Crosnier H, Sulmont V, de Kerdanet M, Scharfmann R, Lebenthal Y, Froguel P, Vaxillaire M, French ND (Neonatal Diabetes) Study Group. Heterozygous missense mutations in the insulin gene are linked to permanent diabetes appearing in the neonatal period or in early infancy: a report from the French ND (Neonatal Diabetes) Study Group. Diabetes 2008;57:1115–1119
11. Molven A, Ringdal M, Nordbø AM, Raeder H, Støy J, Lipkind GM, Steiner DF, Philipson LH, Bergmann I, Aarskog D, Undlien DE, Joner G, Søvik O, Norwegian Childhood Diabetes Study Group, Bell GI, Njølstad PR. Mutations in the insulin gene can cause MODY and autoantibody-negative type 1 diabetes. Diabetes 2008;57:1131–1135
12. Colombo C, Porzio O, Liu M, Massa O, Vasta M, Salardi S, Beccaria L, Monciotti C, Toni S, Pedersen O, Hansen T, Federici L, Pesavento R, Cadario F, Federici G, Ghirri P, Arvan P, Iafusco D, Barbetti F, Early Onset Diabetes Study Group of the Italian Society of Pediatric Endocrinology and Diabetes (SIEDP). Seven mutations in the human insulin gene linked to permanent neonatal/infancy-onset diabetes mellitus. J Clin Invest 2008;118:2148–2156
13. Bonfanti R, Colombo C, Nocerino V, Massa O, Lampasona V, Iafusco D, Viscardi M, Chiumello G, Meschi F, Barbetti F. Insulin gene mutations as cause of diabetes in children negative for five type 1 diabetes autoantibodies. Diabetes Care 2009;32:123–125
14. Tarasov AI, Nicolson TJ, Riveline JP, Taneja TK, Baldwin SA, Baldwin JM, Charpentier G, Gautier JF, Froguel P, Vaxillaire M, Rutter GA. A rare mutation in ABCC8/SUR1 leading to altered ATP-sensitive K+ channel activity and beta-cell glucose sensing is associated with type 2 diabetes in adults. Diabetes 2008;57:1595–1604
15. Liu M, Hodish I, Rhodes CJ, Arvan P. Proinsulin maturation, misfolding, and proteotoxicity. Proc Natl Acad Sci U S A 2007;104:15841–15846
16. Chèvre JC, Hani EH, Boutin P, Vaxillaire M, Blanché H, Vionnet N, Pardini VC, Timsit J, Larger E, Charpentier G, Beckers D, Maes M, Bellanné-Chantelot C, Velho G, Froguel P. Mutation screening in 18 Caucasian families suggest the existence of other MODY genes. Diabetologia 1998;41:1017–1023
17. Miyazaki J, Araki K, Yamato E, Ikegami H, Asano T, Shibasaki Y, Oka Y, Yamamura K. Establishment of a pancreatic beta cell line that retains glucose inducible insulin secretion: special reference to expression of glucose transporter isoforms. Endocrinology 1990;127:126–132
18. Tsuboi T, Rutter GA. Multiple forms of "kiss-and-run" exocytosis revealed by evanescent wave microscopy. Curr Biol 2003;13:563–567
19. Varadi A, Cirulli V, Rutter GA. Mitochondrial localization as a determinant of capacitative Ca2+ entry in HeLa cells. Cell Calcium 2004;36:499–508
20. Ron D, Walter P. Signal integration in the endoplasmic reticulum unfolded protein response. Nat Rev Mol Cell Biol 2007;8:519–529
21. Cnop M, Welsh N, Jonas JC, Jorns A, Lenzen S, Eizirik DL. Mechanisms of pancreatic beta-cell death in type 1 and type 2 diabetes: many differences, few similarities. Diabetes 2005;54(Suppl. 2):S97–S107
22. Cunha DA, Hekerman P, Ladrière L, Bazarra-Castro A, Ortis F, Wakeham MC, Moore F, Rasschaert J, Cardozo AK, Bellomo E, Overbergh L, Mathieu C, Lupi R, Hai T, Herchuelz A, Marchetti P, Rutter GA, Eizirik DL, Cnop M. Initiation and execution of lipotoxic ER stress in pancreatic beta cells. J Cell Sci 2008;121:2308–2318
23. Oyadomari S, Mori M. Roles of CHOP/GADD153 in endoplasmic reticulum stress. Cell Death Differ 2004;11:381–389
24. Lai E, Bikopoulos G, Wheeler MB, Rozakis-Adcock M, Volchuk A. Differential activation of ER stress and apoptosis in response to chronically elevated free fatty acids in pancreatic beta-cells. Am J Physiol Endocrinol Metab 2008;294:E540–E550
25. Glaser B. Insulin mutations in diabetes: the clinical spectrum. Diabetes 2008;57:799–800
26. von Heijne G. Signal sequences: the limits of variation. J Mol Biol 1985;184:99–105
27. von Heijne G. Analysis of the distribution of charged residues in the N-terminal region of signal sequences: implications for protein export in prokaryotic and eukaryotic cells. EMBO J 1984;3:2315–2318
28. Scheuner D, Kaufman RJ. The unfolded protein response: a pathway that links insulin demand with beta-cell failure and diabetes. Endocr Rev 2008;29:317–333
29. Song B, Scheuner D, Ron D, Pennathur S, Kaufman RJ. Chop deletion reduces oxidative stress, improves beta cell function, and promotes cell survival in multiple mouse models of diabetes. J Clin Invest 2008;118:3378–3389
30. Smith GD, Pangborn WA, Blessing RH. The structure of T6 human insulin at 1.0 A resolution. Acta Crystallogr D Biol Crystallogr 2003;59:474–482